30th International Conference
ENGINEERING MECHANICS 2024
Milovy, Czech Republic, May 14 – 16, 2024

INFLUENCE OF SINE-SHAPED PROFILE DEVIATIONS ON STATIC TRANSMISSION ERROR

Rackovský D. M.*, Czakó A.**

Abstract: *Transmission error (TE), a parameter influencing gears vibration and subsequent noise, is a subject addressed in many papers. However, most researchers consider ideal or modified involute while neglecting machining errors. This case study extends the author's previous work (Czakó et al., 2020) by incorporating tooth profile errors and investigating their impact on static transmission error (STE). Parametric geometry of 2D spur gears, including sine-shaped involute profiles, was generated directly within the Ansys Mechanical environment using APDL (Ansys Parametric Design Language), where all finite element analyses (FEA) were conducted. Various amplitudes corresponding to ISO 1328-1 accuracy grades 1–8, and wavelengths of sine functions modulated onto involutes, were simulated and compared in terms of resulting STE. The results underscore the importance of including profile deviations in models, mainly those common in industry, as they significantly influence transmission error.*

Keywords: Static transmission error, machining errors, gears, accuracy grades, finite element analysis.

1. Introduction

Demands on transmission systems, especially in the automotive industry, continue to grow in terms of vibration and noise. Transmission error is a well-known parameter closely related to the vibration and noise of transmission systems (Smith, 2003). Its values and waveforms, depending on the rotation of meshing gears, are influenced by many factors, such as time-varying mesh stiffness (TVMS), stiffness of adjacent components (bearings, shafts, housing), micro-geometric modifications, damages, and lubrication conditions of gear teeth, as well as the presence of assembly and machining errors. Notably, deviations from the theoretical shape of the tooth profile/flank have a significant impact on resulting TE as they may reach similar values, depending on the machining accuracy grade, as the transmission error itself.

Kiekbusch et al. (2011) developed 2D and 3D finite element (FE) models of meshing gear pairs using APDL scripts. Their model included an adaptive meshing algorithm to refine mesh in contacts zones. However, only ideal involute profiles were considered. Lin and He (2017) presented a parametric program for creating helical gears with machining errors in Matlab. Both profile and helix errors were generated by a model of a cutter tool with error represented by sine functions. They concluded that, compared to ideal teeth, both average and peak-to-peak (PTP) TE increased significantly. Liang et al. (2023), who created a FE model of a hypoid gear pair to investigate the impact of measured tooth surface errors on TE and contact pattern, reached a similar conclusion. Liu et al. (2022) developed a mathematical model for TVMS of helical gears with various types of machining errors considering three accuracy grades (4–6) according to ISO standard. Similarly, Guo and Fang (2020) analyzed random tooth profile and pitch errors (grades 5–7) and their influence on vibrational response of meshing helical gears. Hjelm et al. (2021) examined at spur gears the relationship between static transmission error (STE), contact pressure, and manufacturing tolerances commonly used in the automotive industry (grades 5–8) for spur gears. The results were transmission error curves for various combinations of pitch and tooth profile slope errors.

* Bc. Daniel Milan Rackovský: Institute of Automotive Engineering, Brno University of Technology, Technicka 2896/2; 61669, Brno; CZ, 217568@vutbr.cz

** Ing. Alexander Czakó: Institute of Automotive Engineering, Brno University of Technology, Technicka 2896/2; 61669, Brno; CZ, alexander.czako@vutbr.cz

doi: 10.21495/em2024-246

2. Methods

2.1. Parametric geometry

The geometry of the 2D spur gear pair was created using APDL in Ansys Mechanical. The script developed for this purpose consisted of input parameters for the gears, equations for macro-geometry, and profile errors represented by sine functions. These sine functions were modulated onto the involutes by adding them in the normal direction of the involute. Additionally, the root fillet curve was defined by the trochoid equation (Mohammed, 2023). The model also allows for the addition of tip chamfer. To ensure transitions between curves, the minimum and maximum values of parameters for construction of each curve were computed. Other teeth were created by rotating the curves about the gear center. An arbitrary number of teeth can be chosen; in this study, it was five on each gear. Using these equations of the curves, coordinates of keypoints were determined enabling the creation of closed areas for the gears. Moreover, the gears were rotated until the teeth just touched.

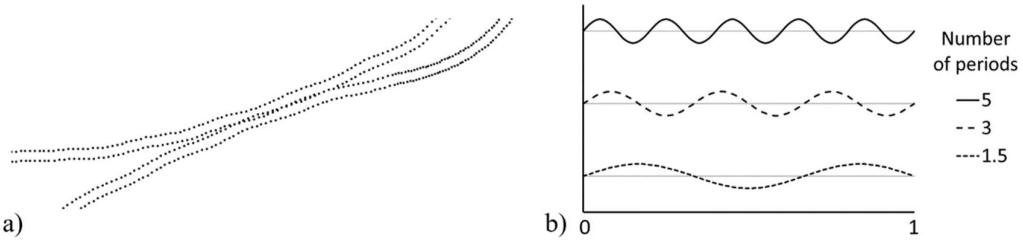

Fig. 1: Profile deviations: a) created by keypoints, b) schematic (0 – start, 1 – end of the involute).

In this study, one set of macro-geometry parameters was considered for further analysis. Specifically, normal module of 2.5 mm, number of teeth of 21 and 32, pressure angle of 20 °, addendum coefficient of 1, tip clearance coefficient of 0.25, working center distance of 66.3 mm, and tip chamfer of 0.3 mm × 45 °. The gear pair differed only in micro-geometry – sine wavelength (see Fig. 1b) and PTP amplitude which was determined by total profile tolerance in the given grade (see Tab. 1). All teeth of a single gear pair were modeled with identical profile deviations.

Grade	1st	2nd	3rd	4th	5th	6th	7th	8th
Profile tolerance (total) [µm]	2	2.9	4.1	6	8	12	16	23

Tab. 1: Profile tolerances (total) for different accuracy grades according to ISO 1328-1.

2.2. Finite element analysis

Numerical simulations of the gear engagement were carried out in the same environment as the generation of geometry, which is advantageous in terms of shorter preprocessing time. Firstly, the finite element mesh was generated based on the keypoints, where the keypoints defined positions of the nodes. The keypoints along the involutes and trochoids were offset into the gear to create a layer, which was then meshed by square elements PLANE183 (see Fig. 2) considering plane strain. The element size, the distance between corresponding keypoints, of these layers was set to be relatively small to capture the curvature precisely. Based on the sensitivity study, the element size of 0.05 mm, and layer width of two elements were chosen.

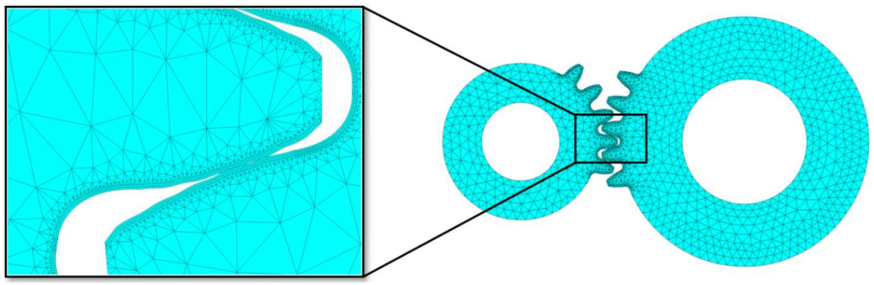

Fig. 2: Finite element mesh of the gears.

The gears were constrained at their centers, allowing only one rotational degree of freedom about their axes. The driven gear was loaded with a moment of 20 N.m, while the driving one was defined to rotate by 30 °, with an increment of 0.1 °, to capture more than one period of the TE. Surface-to-surface contact

between the meshing teeth was ensured by contact elements CONTA172 and TARGE169. The contact settings remained consistent throughout all simulations, with the friction coefficient of 0.1, the normal contact stiffness factor and penetration tolerance factor of 1. The Augmented Lagrange method was used.

Based on the results of stress-strain contact analysis (see Fig. 3), the static transmission error was subsequently calculated from the definition as follows (Smith, 2003):

$$STE = r_1\theta_1 - r_2\theta_2 \tag{1}$$

where r is pitch circle radius, θ is angular displacement (in radians) of the gear center, and indexes 1 and 2 refer to the driving and driven gear, respectively.

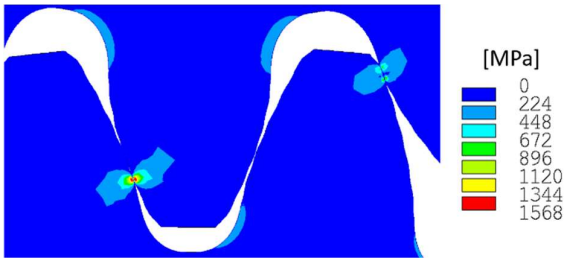

Fig. 3: Equivalent stress von-Mises in loaded teeth of meshing gears.

3. Results and discussion – static transmission error

The resulting graphs of the static transmission error are shown in Fig. 4, where the accuracy grades are compared for each number of periods of the sine function. Since spur gears with contact ratio between 1 and 2 were considered, one and two tooth pairs alternated in the mesh. Observing the graph for the ideal involute, higher STE values correspond to the single-pair engagement. Notably, the higher the grade, the more pronounced deviations from the ideal involute graph. However, the way the deviations transform the ideal involute graphs strongly depends on the sine wavelength.

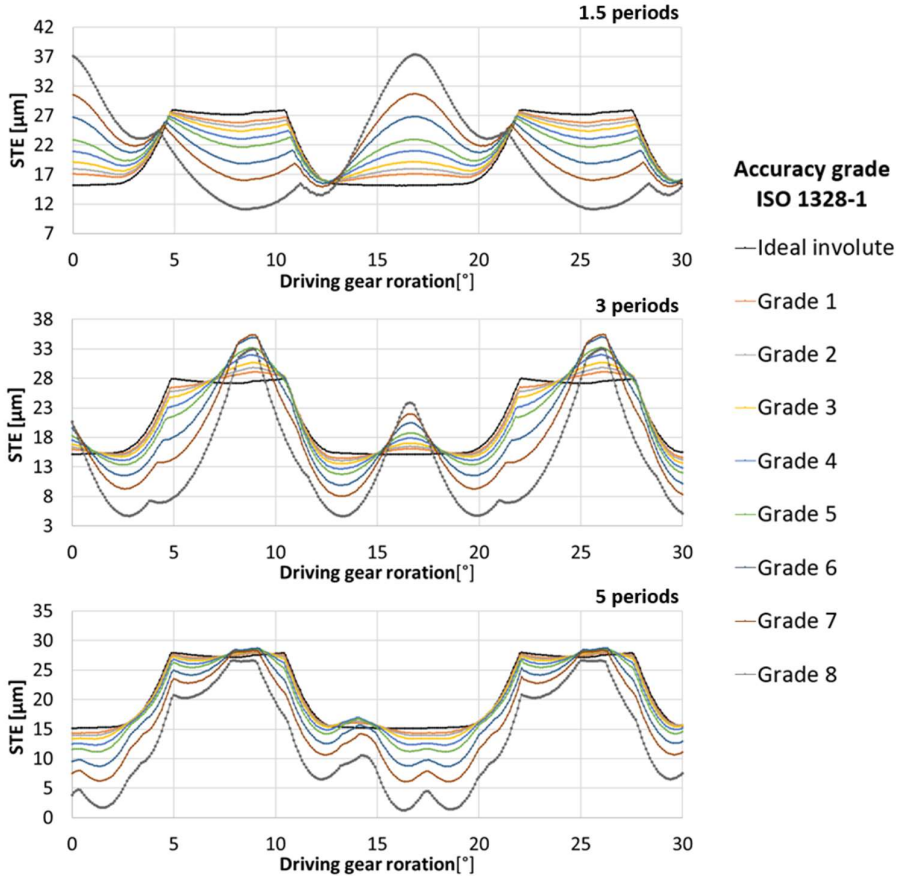

Fig. 4: STE graphs for various numbers of sine periods and ISO accuracy grades.

For the case of 1.5 periods, with the increasing grade, the STE of single-pair engagement decreases while that of two-pair engagement increases. This leads in a slight decrease in the PTP-STE up to the grade 6. However, beyond this point, the values start to increase rapidly (see Fig. 5 – note that the value of zero indicates the ideal involute). As the number of sine periods increases, the waveforms tend to resemble the trend of the ideal involute graph. Furthermore, PTP-STE values grow more gradually with higher grades in the case of 3 and 5 periods reaching similar values to those of 1.5 periods for the grade 8. Specifically, each of them is approximately two times higher than that of the ideal involute. It can be concluded that not only do the grades influence transmission error, but also the way they are distributed along the involutes.

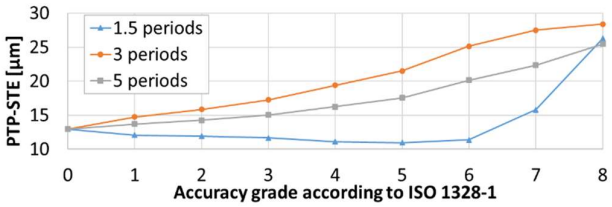

Fig. 5: Comparison of different tooth profiles through accuracy grades in terms of PTP-STE.

4. Conclusions

The case study presented in this paper focuses solely on 2D tooth profiles. While this approach offers the advantage of shorter computational times, it also means that flank line deviations and modifications, and helical gears cannot be incorporated. Therefore, future plans involve extending the FEM model to include 3D representations. Additionally, there is potential to enhance fidelity of the simulation by considering more complex curves beyond simple sine shapes and defining different deviations across the teeth to better reflect real-world conditions. This may also help to improve dynamic models (Otipka et al., 2019) and (Prokop and Řehák, 2017) of geared transmission systems by providing more realistic transmission error waveforms, considering inevitable machining errors, as the input.

Acknowledgement

The research leading to these results has received funding from the project Specific research on BUT FSI-S-20-6267. The authors gratefully acknowledge this support.

References

Czakó, A., Řehák K. and Prokop A. (2020) Determination of transmission error at helical gear. In: *Proc. of 26th Engineering Mechanics*, Brno, pp. 118–121.

Guo, F. and Fang, Z. (2020) The statistical analysis of the dynamic performance of a gear system considering random manufacturing errors under different levels of machining precision. *Proc. of the Institution of Mechanical Engineers*, Part K: Journal of Multi-body Dynamics, 234, 1, pp. 3–18.

Hjelm, R., Ahadi, A. and Wahlström, J. (2021) Gear tolerancing for simultaneous optimization of transmission error and contact pressure. *Results in Engineering*, 9, pp. 1–8.

Kiekbusch, T., Sappok, D., Sauer, B. and Howard, I. (2011) Calculation of the Combined Torsional Mesh Stiffness of Spur Gears with Two- and Three-Dimensional Parametrical FE Models. Strojniški vestnik - *Journal of Mechanical Engineering*, 57, 11, pp. 810–818.

Liang, Ch., Song, Ch., Zhu, C. and Liu, S. (2023) Modelling method, simulation and experimental verification of hypoid gear involved tooth surface deviation under manufacturing process. *Mechanism and Machine Theory*, 182, pp. 1–19.

Lin, T. and He, Z. (2017) Analytical method for coupled transmission error of helical gear system with machining errors, assembly errors and tooth modifications. *Mechanical Systems and Signal Processing*, 91, pp. 167–182.

Liu, Ch., Shi, W. and Liu, K. (2022) Calculation method of mesh stiffness for helical gear pair with manufacturing errors, assembly errors and tooth modifications. *Meccanica*, 57, 3, pp. 541–565.

Mohammed, O. D. (2023) An analytical approach for the determination of helical gear tooth geometry. *Journal of Engineering, Design and Technology*, pp. 1–23.

Otipka, V., Zajac, R., Řehák, K. and Prokop, A. (2019) Numerical dynamic analysis of gearbox behaviour. *Acoustics and Vibration of Mechanical Structures*, 25, pp. 433–441.

Prokop, A. and Řehák, K. (2017) Virtual prototype application to heavy-duty vehicle gearbox concept. In: *Proc. of 23rd Engineering Mechanics*, Svratka, pp. 810–813.

Smith, J. D. (2003) *Gear noise and vibration*. 2nd edition. New York: Marcel Dekker.